Estimation of Object Reflectance Spectra from Digital Camera Images

Takayuki Hasegawa[1,2] *and Mark D. Fairchild*[2]
[1]*Technical Research Institute, Toppan Printing Co., Ltd., Saitama, Japan*
[2]*Munsell Color Science Laboratory, RIT, Rochester, New York, USA*

Abstract

Digital cameras are often used as colorimeters where the task is to predict as accurate colorimetric values of an object as possible from camera responses of the object. It has been widely recognized that one of the factors that makes color prediction less straightforward is metamerism.

This paper addresses a novel color prediction method that utilizes a population of spectral reflectance samples of real objects based on which the effect of metamerism is taken into consideration. The results of computer simulations show that the proposed method is able to achieve higher performance than the conventional matrix-based color prediction method.

Introduction

As the performance of digital cameras has been significantly improved in terms of both image quality and spatial resolution, they have been incorporated into a sequence of color reproduction systems where the critical issue is the consistency of color from the original scene through the color rendering devices. The task of manipulating digital camera images in this case is to predict colorimetric values of an object in the scene as accurately as possible from camera responses of the object. It has been widely recognized that one of the factors that makes color prediction less straightforward is metamerism. That is, a pair of surface reflectances are recorded as the identical camera responses but have different colorimetric values due to the fact that spectral sensitivities of a camera generally differ from those of the human visual system. Another aspect of metamerism is that the illuminant used to capture an image is not necessarily the same as the illuminant under which the color of the object should be predicted.

It is obvious that the simplest way of color prediction using a 3×3 transformation matrix that relates camera responses with CIE tristimulus values fails to achieve acceptable performance due to metamerism except in some special cases. Although attempts have been made to improve the color prediction accuracy by adding higher polynomials and a constant term to the transformation matrix,[1,2] it does not mean that such approaches take metamerism into account effectively.

This paper describes a new method to predict the color of an object from digital camera responses in consideration of metamerism and evaluates its performance compared with a conventional color prediction method by means of computer simulations.

Color Prediction Methods

Matrix-based Color Prediction

The color of an object is specified as Eq. (1) by evenly sampling spectral data at N points over the visible range:

$$\mathbf{t}_{XYZ} = \mathbf{F}_{XYZ}^{\mathrm{T}} \mathbf{E}_v \mathbf{r} \tag{1}$$

where $\mathbf{t}_{XYZ}$ is a 3×1 vector of CIE tristimulus values, $\mathbf{F}_{XYZ}$ is an $N \times 3$ matrix of CIE color matching functions, $\mathbf{E}_v$ is an $N \times N$ diagonal matrix of the spectrum of the illuminant under which the object is observed, and $\mathbf{r}$ is an $N \times 1$ vector of the object reflectance.

Sensor responses of the object from a three-channel camera can be expressed as:

$$\mathbf{t}_{RGB} = \mathbf{F}_{RGB}^{\mathrm{T}} \mathbf{E}_t \mathbf{r}, \tag{2}$$

where $\mathbf{t}_{RGB}$ is a 3×1 vector of the sensor responses, typically R, G, and B, $\mathbf{F}_{RGB}$ is an $N \times 3$ matrix composed of three camera sensitivities, and $\mathbf{E}_t$ is an $N \times N$ diagonal matrix of illuminant spectrum employed for image capturing.

The conventional color prediction utilizes a linear transformation as described in Eq. (3):

$$\hat{\mathbf{t}}_{XYZ} = \mathbf{L}_{3\times3} \mathbf{t}_{RGB}, \tag{3}$$

where $\hat{\mathbf{t}}_{XYZ}$ is the estimation of the tristimulus values and $\mathbf{L}_{3\times3}$ is a 3×3 transformation matrix. There are two primary ways of theoretically determining the transformation matrix $\mathbf{L}_{3\times3}$.

The first method is based on the characteristic of reflectance spectra. Suppose a collection of reflectance spectra spans a subspace whose dimension is no more than

three. Principal component analysis[3–5] is most often employed to determine orthonormal basis vectors $\mathbf{b}_i\,(i = 1,\,2,\,3)$ in this space that enables any spectrum to be specified as a linear reflectance model[3–11] represented in Eq. (4):

$$\mathbf{r} = \sum_{i=1}^{3} w_i \mathbf{b}_i = \mathbf{B}\mathbf{w}, \tag{4}$$

where w_i is a coefficient for the basis vector $\mathbf{b}_i$, $\mathbf{B}$ is an $N \times 3$ matrix composed of the basis vectors, and $\mathbf{w}$ is a 3×1 vector of the coefficients. From Eqs. (2) and (4),

$$\mathbf{t}_{RGB} = \mathbf{F}_{RGB}^{\mathrm{T}} \mathbf{E}_t \mathbf{B}\mathbf{w}. \tag{5}$$

Since the matrix product $\mathbf{F}_{RGB}^{\mathrm{T}} \mathbf{E}_t \mathbf{B}$ yields a 3×3 square matrix, the reflectance vector $\mathbf{r}$ can be derived from Eqs. (4) and (5):

$$\mathbf{r} = \mathbf{B}(\mathbf{F}_{RGB}^{\mathrm{T}} \mathbf{E}_t \mathbf{B})^{-1} \mathbf{t}_{RGB}. \tag{6}$$

Substituting Eq. (6) for Eq. (1), the 3×3 transformation matrix $\mathbf{L}_{3\times3}$ is defined as:

$$\mathbf{L}_{3\times3} = \mathbf{F}_{XYZ}^{\mathrm{T}} \mathbf{E}_v \mathbf{B}(\mathbf{F}_{RGB}^{\mathrm{T}} \mathbf{E}_t \mathbf{B})^{-1}. \tag{7}$$

The shortcoming of this model is that object spectra existing in the real world span a more than three-dimensional subspace. Under the assumption of Eq. (4), tristimulus values $\mathbf{t}_{XYZ}$ can be uniquely derived from $\mathbf{t}_{RGB}$ because there is only one reflectance spectrum that gives the specified sensor responses $\mathbf{t}_{RGB}$. However, in case more than three dimensions are required for the complete spectral reconstruction, a unique solution cannot be found since multiple reflectances that yield different $\mathbf{t}_{XYZ}$ could give the same $\mathbf{t}_{RGB}$ (those reflectances are referred to as camera-metamers hereafter). It has been found that the spectral reconstruction accuracy of the three-dimensional linear reflectance model is comparatively high for some specific object categories such as human skin and vegetation.[10,12,13] More than three dimensions are required to achieve sufficient accuracy for other types of objects.[7,8,11]

The second approach focuses on the spectral property of both the human perception and the image capturing system. If $\mathbf{F}_{XYZ}\mathbf{E}_v$ spans the same three-dimensional subspace as $\mathbf{F}_{RGB}\mathbf{E}_t$, $\mathbf{F}_{XYZ}\mathbf{E}_v$ can be expressed as a linear transformation of $\mathbf{F}_{RGB}\mathbf{E}_t$:

$$\mathbf{F}_{XYZ}\mathbf{E}_v = \mathbf{L}_{3\times3}\mathbf{F}_{RGB}\mathbf{E}_t. \tag{8}$$

In this case, there could be multiple spectral reflectances corresponding to the specified $\mathbf{t}_{RGB}$. However, it does not matter since they all give the same $\mathbf{t}_{XYZ}$. Generally, Eq. (8) hardly holds perfectly due to the practical limitations in manufacturing the desired camera sensitivities. Furthermore, even if it is possible to fabricate the camera sensitivities optimal for a fixed pair of viewing and taking illuminants, the lighting conditions are likely to change in the use of digital cameras and Eq. (8) no longer holds. In such cases, it is impossible to relate the specified $\mathbf{t}_{RGB}$ with a unique $\mathbf{t}_{XYZ}$ because of camera-metamerism. The transformation matrix $\mathbf{L}_{3\times3}$ is therefore determined by the least-squares method:

$$\begin{aligned} \mathbf{L}_{3\times3} \;=\; & \mathbf{F}_{XYZ}^{\mathrm{T}} \mathbf{E}_v (\mathbf{F}_{RGB}^{\mathrm{T}} \mathbf{E}_t)^{\mathrm{T}} \\ & \times \{\mathbf{F}_{RGB}^{\mathrm{T}} \mathbf{E}_t (\mathbf{F}_{RGB}^{\mathrm{T}} \mathbf{E}_t)^{\mathrm{T}}\}^{-1}. \end{aligned} \tag{9}$$

Color prediction accuracy based on the transformation matrix defined in Eq. (9) depends on how far the subspace spanned by $\mathbf{F}_{RGB}\mathbf{E}_t$ departs from that spanned by $\mathbf{F}_{XYZ}\mathbf{E}_v$. Vora and Trussell have introduced μ-factor,[14] a metric for the colorimetric evaluation of image capturing systems, as an extension of Neugebauer's q-factor.[15]

Since either model has a prerequisite condition which is not always satisfied, the transformation matrix $\mathbf{L}_{3\times3}$ is sometimes determined by the linear regression method using a set of color samples whose $\mathbf{t}_{XYZ}$ and $\mathbf{t}_{RGB}$ are known. Cross terms and a constant term are also often introduced to the regression procedure in order to compensate for the nonlinearity between $\mathbf{t}_{RGB}$ and $\mathbf{t}_{XYZ}$:

$$\hat{\mathbf{t}}_{XYZ} = \mathbf{L}_{3\times8}\,[R,\,G,\,B,\,RG,\,GB,\,BR,\,RGB,\,1]^{\mathrm{T}}, \tag{10}$$

where $\mathbf{L}_{3\times8}$ is a 3×8 transformation matrix. Although this model can to some extent improve the performance of color prediction, there still remains a defect that it does not efficiently minimize the effect of camera-metamers.

High-Dimensional Reflectance Estimation

As indicated in the previous section, taking account of camera metamerism is one of the essential factors to improve color prediction accuracy. Since camera metamerism is caused by the higher-dimensional reflectance subspace, it is reasonable to extend the linear reflectance model to n dimensions:

$$\mathbf{r} = \sum_{i=1}^{n} w_i \mathbf{b}_i = \mathbf{B}\mathbf{w}. \tag{11}$$

In case $n > 3$, both the basis matrix $\mathbf{B}$ and the coefficient vector $\mathbf{w}$ can be divided into two parts as follows:

$$\begin{aligned} \mathbf{B} &= [\mathbf{B}_l,\,\mathbf{B}_h], \\ \mathbf{w} &= [\mathbf{w}_l^{\mathrm{T}},\,\mathbf{w}_h^{\mathrm{T}}]^{\mathrm{T}}, \\ \mathbf{B}_l &= [\mathbf{b}_1,\,\mathbf{b}_2,\,\mathbf{b}_3], \\ \mathbf{B}_h &= [\mathbf{b}_4,\,\mathbf{b}_5,\,\cdots,\,\mathbf{b}_n], \\ \mathbf{w}_l &= [w_1,\,w_2,\,w_3]^{\mathrm{T}}, \\ \mathbf{w}_h &= [w_4,\,w_5,\,\cdots,\,w_n]^{\mathrm{T}}. \end{aligned}$$

Using these definitions, the sensor response vector $\mathbf{t}_{RGB}$ in Eq. (2) can be expressed by Eq. (12):

$$\begin{aligned}\mathbf{t}_{RGB} &= \mathbf{F}_{RGB}\mathbf{E}_t\left[\mathbf{B}_l\mathbf{w}_l + \mathbf{B}_h\mathbf{w}_h\right] \\ &= \mathbf{F}_{RGB}\mathbf{E}_t\mathbf{B}_l\mathbf{w}_l + \mathbf{F}_{RGB}\mathbf{E}_t\mathbf{B}_h\mathbf{w}_h \\ &= \mathbf{M}_l\mathbf{w}_l + \mathbf{M}_h\mathbf{w}_h, \end{aligned} \tag{12}$$

where $\mathbf{M}_l = \mathbf{F}_{RGB}\mathbf{E}_t\mathbf{B}_l$ and $\mathbf{M}_h = \mathbf{F}_{RGB}\mathbf{E}_t\mathbf{B}_h$. Since $\mathbf{M}_l$ is a 3×3 square matrix, Eq. (12) can be rewritten as:

$$\mathbf{w}_l = {\mathbf{M}_l}^{-1}(\mathbf{t}_{RGB} - \mathbf{M}_h\mathbf{w}_h). \tag{13}$$

The estimation of the spectral reflectance $\hat{\mathbf{r}}$ that gives the sensor response vector $\mathbf{t}_{RGB}$ is therefore described as:

$$\begin{aligned}\hat{\mathbf{r}} &= \mathbf{B}_l\mathbf{w}_l + \mathbf{B}_h\mathbf{w}_h \\ &= \mathbf{B}_l{\mathbf{M}_l}^{-1}(\mathbf{t}_{RGB} - \mathbf{M}_h\mathbf{w}_h) + \mathbf{B}_h\mathbf{w}_h \\ &= (\mathbf{B}_h - \mathbf{B}_l{\mathbf{M}_l}^{-1}\mathbf{M}_h)\mathbf{w}_h \\ &\quad + \mathbf{B}_l{\mathbf{M}_l}^{-1}\mathbf{t}_{RGB}. \end{aligned} \tag{14}$$

For a given sensor response vector $\mathbf{t}_{RGB}$, only the vector $\mathbf{w}_h$ is the variable term in Eq. (14) because the matrices $\mathbf{B}_l$, $\mathbf{B}_h$, $\mathbf{M}_l$, and $\mathbf{M}_h$ are all known. Defining $\mathbf{P} = \mathbf{B}_h - \mathbf{B}_l{\mathbf{M}_l}^{-1}\mathbf{M}_h$ and $\mathbf{q} = \mathbf{B}_l{\mathbf{M}_l}^{-1}\mathbf{t}_{RGB}$, Eq. (14) can be simplified as Eq. (15):

$$\hat{\mathbf{r}} = \mathbf{P}\mathbf{w}_h + \mathbf{q}. \tag{15}$$

Equation (15) means that an arbitrary input $\mathbf{w}_h$ yields a camera metamer $\hat{\mathbf{r}}$ that gives the sensor responses $\mathbf{t}_{RGB}$. Allowing vector $\mathbf{w}_h$ to take m discrete inputs $\mathbf{w}_{h,j}$ ($j = 1, 2, \cdots, m$), each input leads to a camera metamer $\hat{\mathbf{r}}_j$. The CIELAB coordinates L_j^*, a_j^*, and b_j^* can be calculated for each $\hat{\mathbf{r}}_j$ and their mean values can be considered to represent the expected object color.

However, it is not guaranteed that the reconstructed spectrum $\hat{\mathbf{r}}$ really exists as a spectral reflectance of the object. For instance, probability of existence of a spectral reflectance is zero if it has a value smaller than 0 or greater than 1. In addition, even if $0 \le \hat{\mathbf{r}} \le 1$, the probability of existence should be estimated lower for $\hat{\mathbf{r}}$ whose characteristics (steepness of the spectral curve shape, number of principal peaks, etc.) significantly departs from those of the real spectrum of the object. It is reasonable to appropriately determine weighting factors ω_j ($j = 1, 2, \cdots, m$) in consideration of the probability of existence of the spectral reflectance $\hat{\mathbf{r}}_j$. With those weighting factors, Eq. (16) represents the expected colorimetric values of the object:

$$\begin{aligned}\hat{L}^* &= \frac{1}{\Omega}\sum_{j=1}^{m}\omega_j L_j^*, \\ \hat{a}^* &= \frac{1}{\Omega}\sum_{j=1}^{m}\omega_j a_j^*, \\ \hat{b}^* &= \frac{1}{\Omega}\sum_{j=1}^{m}\omega_j b_j^*, \\ \Omega &= \sum_{j=1}^{m}\omega_j. \end{aligned} \tag{16}$$

It is desirable to determine the weighting coefficient ω_j based on some spectral characteristics that real objects possess. If the population of spectral reflectance samples used to construct the linear reflectance model of Eq. (11) has a certain tendency that is unique for objects having the same kind of attribute (natural objects, textiles, paints, etc.), ω_j can be determined based on that tendency.

Defining coefficient vectors of the population samples obtained by the n-dimensional linear model as $\dot{\mathbf{w}}_1, \dot{\mathbf{w}}_2, \cdots, \dot{\mathbf{w}}_p$, these vectors can be considered as p points distributed in the n-dimensional space. If the feature of the population samples appears in this distribution, the weighting factor ω_j that reflects the probability of existence of the spectral reflectance $\hat{\mathbf{r}}_j$ can be determined by comparing this distribution with the coefficient vector $\mathbf{w}_j$ which is used to derive $\hat{\mathbf{r}}_j$. The coefficient vector $\mathbf{w}_j$ here is defined as:

$$\mathbf{w}_j = \begin{bmatrix} \mathbf{w}_{l,j} \\ \mathbf{w}_{h,j} \end{bmatrix}, \tag{17}$$

where $\mathbf{w}_{l,j}$ can be obtained by giving $\mathbf{w}_{h,j}$ to Eq. (13).

Let $s_{j,k}$ denote the similarity of $\mathbf{w}_j$ to $\dot{\mathbf{w}}_k$, the coefficient vector of the kth population sample:

$$s_{j,k} = \exp\left\{-\sum_{i=1}^{n}\frac{(\dot{w}_{k,i} - w_{j,i})^2}{\sigma_i^2}\right\}, \tag{18}$$

where $\dot{w}_{k,i}$ and $w_{j,i}$ are the ith element of the coefficient vectors $\dot{\mathbf{w}}_k$ and $\mathbf{w}_j$, respectively, and σ_i^2 is the variance of $\dot{w}_i$ for the entire population samples. The similarity $s_{j,k}$ becomes 1 when two coefficient vectors $\dot{\mathbf{w}}_k$ and $\mathbf{w}_j$ are equal and decreases to 0 as the distance between two points increases. The variance σ_i^2 is used because the range of ith coefficient $\dot{w}_i$ depends on the dimension i. Since the coefficient vector $\dot{\mathbf{w}}_k$ is derived from spectral reflectance samples that really exist, $s_{j,k}$ can be considered to be an index of the probability of existence. Equation (18) merely compares $\mathbf{w}_j$ with one of the population samples. The final weighting factor ω_j is defined by summing $s_{j,k}$ for the entire population samples:

$$\omega_j = \begin{cases} \displaystyle\sum_{k=1}^{p} s_{j,k} & \textit{if } 0 \le \hat{\mathbf{r}}_j \le 1, \\ 0 & \textit{otherwise}. \end{cases} \tag{19}$$

According to Eq. (19), the weighting factor ω_j increases when there are a large number of population samples near $\mathbf{w}_j$ and decreases as $\mathbf{w}_j$ departs from the distribution of

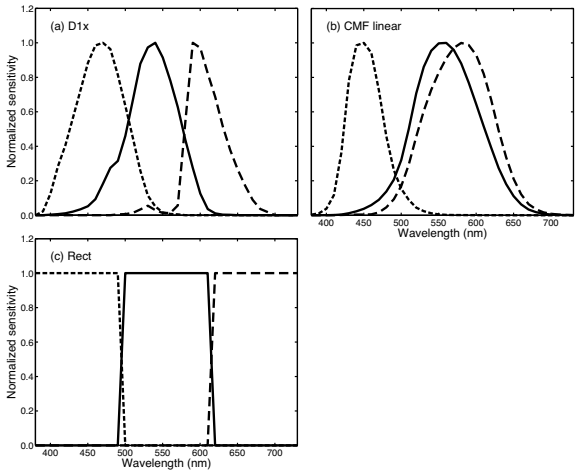

Figure 1: *Spectral sensitivities of a camera used in the simulations. (a) Measurement of a Nikon D1x (RAW format). (b) Linearly transformed from the CIE color matching functions. (c) Synthesized by equi-sensitivity functions.*

population samples. This implies that the weighting factor ω_j reflects the probability of existence of the spectral reflectance $\hat{\mathbf{r}}_j$.

Simulations

A series of simulations was carried out in order to evaluate the performance of the proposed method. CIELAB coordinates of several samples were estimated by the proposed method and were compared with the actual values by means of color difference ΔE^*_{ab}. The color prediction accuracy of the empirical regression method described in Eq. (10) was also evaluated in a similar manner for comparison. Since the regression-based color prediction method yielded negative tristimulus values for some samples, they were clipped to 0.

Through the simulations, all spectral data were sampled at 10 nm intervals in the range of 380-780 nm.

Spectral reflectance data included the measured reflectance of 172 patches of the Macbeth ColorChecker DC and 2832 textile samples from ISO 16066 (SOCS).[16] Although the ColorChecker DC originally consisted of 240 patches, outer 60 gray patches having the same spectral reflectance as the gray patches in the center of the chart and eight patches having a high specular reflectance were removed; therefore, the total number of patches used in the simulations counts 172. Hereafter, the ColorChecker DC spectral reflectance data set is referred to as CCDC F, while the textile data set is referred to as Textile F. In addition, data subsets were created from each data set. CCDC F was randomly divided into two subsets CCDC 1 and CCDC 2 so that each subset had the same number of samples. Similarly, three subsets Textile 1, Textile 2, and Textile 3 were created from Textile F. These data sets and data subsets were utilized as the training data and the test data for both the regression-based color prediction method and the proposed method. The training data were used to determine the matrix $\mathbf{L}_{3\times 8}$ in Eq. (10) for the linear regression method and to perform principal component analysis for the proposed method, while the test data were used to derive color differences.

Table 1: *Dimension of the linear reflectance model v.s. cumulative contribution percentages and mean color differences for the CCDC F and the Textile F data sets.*

Number of bases	CCDC F		Textile F	
	Cum. cont. percentage	Mean ΔE^*_{ab}	Cum. cont. percentage	Mean ΔE^*_{ab}
3	99.3	6.38	97.8	20.06
4	99.7	1.87	99.0	6.67
5	99.8	1.07	99.5	5.49
6	99.9	0.64	99.7	1.73
7	99.9	0.57	99.9	1.15
8	100.0	0.45	99.9	0.53

The CIE D65 illuminant was used as the viewing illuminant, while the measurement of a tungsten lamp was used as the taking illuminant. Figure 1 shows three sets of spectral sensitivities of a camera used in the simulations. Associated with the combination of taking and viewing illuminants used in the simulations, μ-factors were 0.831, 0.969, and 0.559 for D1x, CMF linear, and Rect, respectively.

In order to determine the dimension of the linear reflectance model expressed as Eq. (11), the accuracy of spectral reconstruction was investigated. Table 1 shows the cumulative contribution ratio for each of the CCDC F and the Textile F data sets. Table 1 implies that using six and seven basis vectors is sufficient to achieve the cumulative contribution percentage as high as 99.9% for the CCDC F data set and Textile F data set, respectively. Another inspection was taken in terms of color difference ΔE^*_{ab}. The spectral power distribution of the CIE D65 illuminant, which was used as the viewing illuminant in the simulations, and the CIE color matching functions were applied to the original and reconstructed spectral reflectances and the mean color difference was derived for each data set. The mean color difference is 0.64 with six basis vectors for the CCDC F data set and 1.15 with seven basis vectors for the Textile F data set. According to these results, the dimension of the linear reflectance model was set to six ($n = 6$) and seven ($n = 7$) for each data set and hence the dimension of the vector $\mathbf{w}_h$ which is the input variable

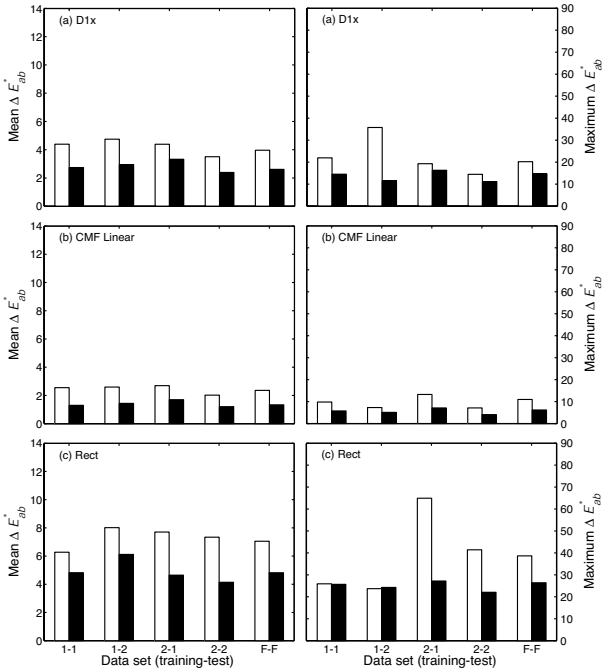

Figure 2: *Color prediction accuracy for the CCDC data sets. White bars show the prediction accuracy of the linear regression method, while black bars represent the proposed method. Labels for the horizontal axis denote the pair of the training data set and the test data set.*

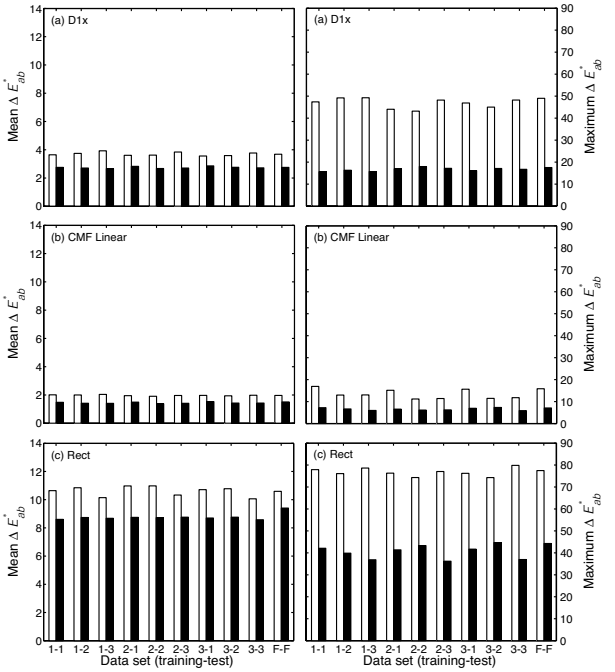

Figure 3: *Color prediction accuracy for the Textile data sets. White bars show the prediction accuracy of the linear regression method, while black bars represent the proposed method. Labels for the horizontal axis denote the pair of the training data set and the test data set.*

to Eq. (15) was correspondingly set to three and four. For the simulations using the ColorChecker DC spectra, three-dimensional grid was created whose jth grid point represented $\mathbf{w}_{h,j}$. Each dimension was evenly sampled with 11 entries so that m, the total number of inputs to Eq. (15), was $1331\,(=11^3)$. Similarly, $14641, (=11^4)$ input variables were determined from a four-dimensional grid with 11 entries for the simulation of textile samples.

Results and Discussion

Figures 2 and 3 show the color prediction accuracy of the proposed method compared with the linear regression method. In all graphs, white bars represent the accuracy of the linear regression method, while the black bars represent the proposed method. Labels on horizontal axes denote the spectral reflectance data sets used as the pair of the training data and the test data.

The evaluation of color prediction accuracy using the CCDC data sets reveals that although the accuracy of the proposed method is higher than, or almost equal to, that of the linear regression method, the degree of the improvement was not highly significant. The possible reason may be the small number of population samples led to the difficulty of making weighting factors to sufficiently reflect the probability of existence of the reconstructed spectral reflectance. However, even when the number of population samples is not large enough, it can be observed that the performance of the proposed method is superior to that of the linear regression method for image capturing systems with a small μ-factor.

In the evaluation using the textile data sets, color prediction accuracy of the proposed method was also higher than the linear regression method. Figure 3 indicates that the proposed method is highly effective for image capturing systems with a small μ-factor. The reason the higher degree of improvement was achieved comparing to the simulations of the CCDC data sets is considered the number of population samples contained in the textile data sets was larger than that of the CCDC data sets. Figure 4 shows examples of the tendency observed in the coefficient w's derived for Textile F data set by Eq. (11). The tendency of the population spectral reflectance samples clearly appears in the plots of coefficient w's and it can be considered to have sufficiently affected the derivation of the weighting factors expressed as Eq. (19). Although same plots were created for CCDC F data set, observed features were less

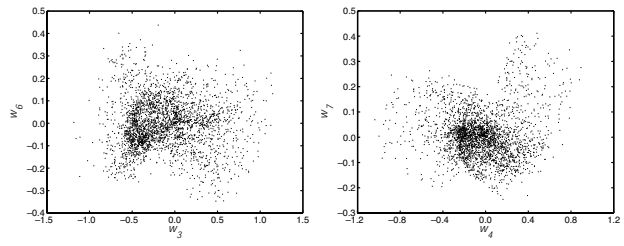

Figure 4: *Distribution plots of coefficient w's which were derived by applying the linear reflectance model to the Textile F data set. The left-hand plot shows w_3 v.s. w_6, while the right-hand plot shows w_4 v.s. w_7.*

significant because the small number of population samples caused sparse distribution.

The camera sensitivity set 'CMF linear' used in the simulations is one of the optimal sets when the taking and viewing illuminants are identical since it is a linear transformation of the color matching functions. However, due to the difference in those two illuminants, the μ-factor departed from 1 and the performance of the linear regression method was rather poor for both simulations with the CCDC and the Munsell data sets. Figures 2 and 3 show that the proposed method was able to achieve about 10-50% smaller color differences.

Evaluating the absolute color difference in Figs. 2 and 3 reveals that the color difference increases as a μ-factor decreases. As mentioned above, the color difference of the linear regression method becomes 0 when the μ-factor is 1. The theory used in the proposed method leads to the fact that the color difference of the proposed method also becomes 0 if the μ-factor is 1. In both methods, the color difference increases as μ-factors decrease. Figures 2 and 3 indicate, however, the proposed method can lessen the degree of increase in color difference comparing to the linear regression method.

Conclusions

A novel method for predicting the color of an object from its camera responses has been presented that utilizes a population of spectral reflectance samples of real objects based on which the effect of camera-metamerism is taken into consideration. A series of computer simulations was carried out in order to examine the performance of the proposed method comparing with a conventional matrix-based color prediction method. Spectral reflectance data of the Macbeth ColorChecker DC and textile samples were employed in the simulations and the color prediction accuracy was evaluated by means of color difference ΔE^*_{ab}. The results revealed that the proposed method is effective especially when the number of population samples is large and can achieve higher performance for image capturing systems with a small μ-factor than the conventional method.

References

1. T. Johnson, Methods for characterizing colour scanners and digital cameras, *Displays*, **16**, 183 (1996).
2. G. Hong, M. R. Luo and P. A. Rhodes, A study of digital camera colorimetric characterization based on polynomial modeling, *Col. Res. Appl.*, **26**, 76 (2001).
3. T. Jaaskelainen, J. Parkkinen and S. Toyooka, Vector-subspace model for color representation, *J. Opt. Soc. Am. A*, **7**, 725 (1990).
4. M. J. Vrhel and H. J. Trussell, Color correction using principal components, *Col. Res. Appl.*, **17**, 328 (1992).
5. H. S. Fairman and M. H. Brill, The principal components of reflectances, *Col. Res. Appl.*, **29**, 104 (2004).
6. L. T. Maloney and B. A. Wandell, Color constancy: A method for recovering surface spectral reflectance, *J. Opt. Soc. Am. A*, **3**, 29 (1986).
7. L. T. Maloney, Evaluation of linear models of surface spectral reflectance with small numbers of parameters, *J. Opt. Soc. Am. A*, **3**, 1673 (1986).
8. J. P. S. Parkkinen, J. Hallikainen and T. Jaaskelainen, Characteristic spectra of munsell colors, *J. Opt. Soc. Am. A*, **6**, 318 (1989).
9. D. H. Marimont and B. A. Wandell, Linear models of surface and illuminant spectra, *J. Opt. Soc. Am. A*, **9**, 1905 (1992).
10. J. L. Dannemiller, Spectral reflectance of natural objects: how many basis functions are necessary?, *J. Opt. Soc. Am. A*, **9**, 507 (1992).
11. M. J. Vrhel, Ron Gershon and L. S. Iwan, Measurement and analysis of object reflectance spectra, *Col. Res. Appl.*, **19**, 4 (1994).
12. C. Chiao and T. W. Cronin, Color signals in natural scenes: characteristics of reflectance spectra and effects of natural illuminants, *J. Opt. Soc. Am. A*, **17**, 218 (2000).
13. Q. Sun and M. D. Fairchild, Statistical characterization of face spectral reflectances and its application to human portraiture spectral estimation, J. *Imaging Sci. Technol.*, **46**, 498 (2002).
14. P. L. Vora and H. J. Trussell, Measure of goodness of a set of color-scanning filters, *J. Opt. Soc. Am. A*, **10**, 1499 (1993).
15. H. E. J. Neugabauer, Quality factor for filters whose spectral transmittances are different from color mixture curves, *J. Opt. Soc. Am.*, **46**, 193 (1983).
16. ISO, Graphic technology — standard object colour spectra database for colour reproduction evaluation (SOCS), Tech. rep., International Standard Organization (2003).

Biography

Takayuki Hasegawa received his B.E. and M.E. degrees from Chiba University, Japan in 1996 and 1998, respectively. He joined Toppan Printing Co., Ltd. in 1998 to work on the development of color management systems. Since 2002, he has been a visiting scientist at Munsell Color Science Laboratory, Center for Imaging Science, Rochester Institute of Technology.